

FC  
4365

Open-file Report 79-926

Open-file Report 79-926

UNITED STATES  
DEPARTMENT OF THE INTERIOR  
GEOLOGICAL SURVEY

Mail Stop 954, Federal Center, Box 25046  
Denver, Colorado 80225

MAJOR-ELEMENT GEOCHEMISTRY OF THE SILENT CANYON-BLACK MOUNTAIN PERALKALINE  
VOLCANIC CENTERS, NORTHWESTERN NEVADA TEST SITE: APPLICATIONS TO  
AN ASSESSMENT OF RENEWED VOLCANISM

By

Bruce M. Crowe<sup>1</sup> and Kenneth A. Sargent<sup>2</sup>

**UNIVERSITY OF UTAH  
RESEARCH INSTITUTE  
EARTH SCIENCE LAB.**

---

<sup>1</sup>Los Alamos Scientific Laboratory, Los Alamos, N. Mex.  
<sup>2</sup>U.S. Geological Survey, Denver, Colo.

## CONTENTS

	Page
Abstract-----	1
Introduction-----	1
Silent Canyon volcanic center-----	3
Geologic setting and evolution-----	3
Age of Silent Canyon volcanic center-----	4
Major-element geochemistry: Silent Canyon-----	4
Black Mountain volcanic center-----	11
Geologic setting and evolution-----	11
Age of Black Mountain volcanic center-----	13
Major-element geochemistry: Black Mountain-----	14
Geochemical comparison: Black Mountain-Silent Canyon centers-----	18
Volcanic hazards: Nevada nuclear waste storage investigations-----	22
References Cited-----	24

## ILLUSTRATIONS

	Page
Figure 1.--Index map of the Nevada Test Site region showing the location of Silent Canyon and Black Mountain volcanic centers-----	2
2.--Major-element oxide plots showing $K_2O$ , $Na_2O$ , and $K_2O+Na_2O$ versus $SiO_2$ for rocks of the Silent Canyon volcanic center-----	6
3.--Major-element oxide plots showing $CaO$ , $MgO$ , and $TiO_2$ versus $SiO_2$ for rocks of the Silent Canyon volcanic center-----	7
4.--Major-element oxide plots showing total iron (as $FeO+0.9 Fe_2O_3$ ) and $Al_2O_3$ versus $SiO_2$ for rocks of the Silent Canyon volcanic center-----	8
5.--Peralkalinity plot versus $SiO_2$ for rocks of the Silent Canyon volcanic center-----	9
6.--Plot of total iron ( $FeO+0.9 Fe_2O_3$ ) versus normative quartz for rocks of the Silent Canyon volcanic center-----	10
7.--Plot of $Al_2O_3$ versus normative quartz for rocks of the Silent Canyon volcanic center-----	12
8.--Major-element oxide plots showing $K_2O$ , $Na_2O$ , and $K_2O+Na_2O$ versus $SiO_2$ for rocks of the Black Mountain volcanic center-----	15
9.--Major-element oxide plots showing $CaO$ , $MgO$ , and $TiO_2$ versus $SiO_2$ for rocks of the Black Mountain volcanic center-----	16
10.--Major-element oxide plots showing total iron (as $FeO+0.9 Fe_2O_3$ ) and $Al_2O_3$ versus $SiO_2$ for rocks of the Black Mountain volcanic center-----	17
11.--Peralkalinity plot versus $SiO_2$ for rocks of the Black Mountain volcanic center-----	19
12.--Plot of total iron ( $FeO+0.9 Fe_2O_3$ ) versus normative quartz for rocks of the Black Mountain volcanic center-----	20
13.--Plot of $Al_2O_3$ versus normative quartz for rocks of the Black Mountain volcanic center-----	21

Mail Stop 954, Federal Center, Box 25046  
Denver, Colorado 80225MAJOR-ELEMENT GEOCHEMISTRY OF THE SILENT CANYON-BLACK MOUNTAIN PERALKALINE  
VOLCANIC CENTERS, NORTHWESTERN NEVADA TEST SITE: APPLICATIONS TO  
AN ASSESSMENT OF RENEWED VOLCANISM

By

Bruce M. Crowe and Kenneth A. Sargent

## ABSTRACT

The Silent Canyon and Black Mountain volcanic centers are located in the northern part of the Nevada Test Site. The Silent Canyon volcanic center is a buried cauldron complex of Miocene age (13-15 m.y.). Black Mountain volcanic center is an elliptical-shaped cauldron complex of late Miocene age.

The lavas and tuffs of the two centers comprise a subalkaline-peralkaline association. Rock types range from quartz normative subalkaline trachyte and rhyolite to peralkaline comendite. The Gold Flat Member of the Thirsty Canyon Tuff (Black Mountain) is a pantellerite.

The major-element geochemistry of the Black Mountain-Silent Canyon volcanic centers differs in the total range and distribution of  $\text{SiO}_2$ , contents, the degree of peralkalinity (molecular  $\text{Na}_2\text{O}+\text{K}_2\text{O} > \text{Al}_2\text{O}_3$ ) and in the values of total iron and alumina through the range of rock types. These differences indicate that the suites were unrelated and evolved from differing magma bodies.

The Black Mountain volcanic cycle represents a renewed phase of volcanism following cessation of the Timber Mountain-Silent Canyon volcanic cycles. Consequently, there is a small but numerically incalculable probability of recurrence of Black Mountain-type volcanism within the Nevada Test Site region. This represents a potential risk with respect to deep geologic storage of high-level radioactive waste at the Nevada Test Site.

## INTRODUCTION

The NTS (Nevada Test Site) is located within the south-central part of the Great Basin, an area of extensive Cenozoic volcanism. An evaluation of time-space patterns of Cenozoic volcanism within the Great Basin (Stewart and Carlson, 1976) suggests a progressive waning in volume and increasingly restricted areal distribution of volcanism within the last 6 m.y. The youngest large-volume volcanic cycle of the NTS region, which is located within the southern Great Basin area, includes the subalkaline-peralkaline Black Mountain volcanic center (Noble and Christiansen, 1974). The relatively large volume of volcanic rocks associated with this center and the explosive nature of eruptive activity suggest the possibility that Black Mountain volcanism or volcanism related to the Black Mountain cycle could pose a risk to long-term geologic storage of radioactive waste within the NTS boundaries.

Three peralkaline volcanic centers are present within central Nevada along an apparent east-west-trending alignment that cuts across the northern part of the NTS (fig. 1). From

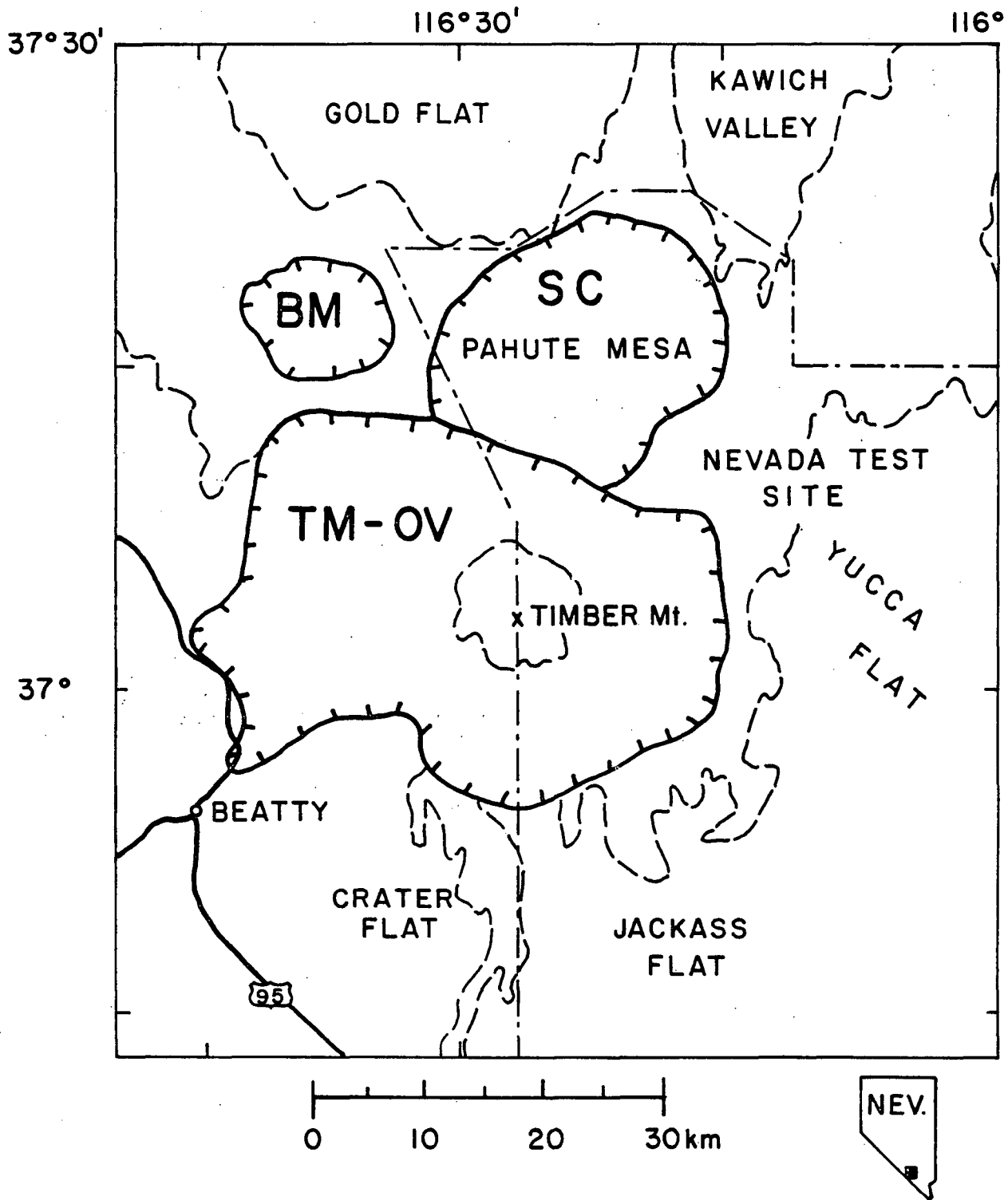


Figure 1.--index map of the Nevada Test Site region showing the location of Silent Canyon (SC) and Black Mountain (BM) volcanic centers. The Timber Mountain-Oasis Valley caldera complex (TM-OV). Hachures outline caldera margins. Dashed lines outline general geographic features.

west to east, the centers include the Black Mountain center, the Silent Canyon center that in part overlaps with the Timber Mountain-Oasis Valley caldera complex (Byers and others, 1976) and the Kane Springs Wash center which lies outside the NTS boundaries (Noble, 1968a; Noble and Parker, 1974). The purpose of this study is to compare the major-element geochemistry of the Black Mountain-Silent Canyon volcanic centers and evaluate geologic evidence related to the possibility of recurrence of silicic volcanism within the NTS region. In the following sections of the paper, we describe and illustrate the geologic setting and major-element geochemistry of the volcanic centers. These data suggest that the Black Mountain and Silent Canyon centers are distinctly separate and evolved from unrelated magma bodies.

## SILENT CANYON VOLCANIC CENTER

### Geologic Setting and Evolution

The Silent Canyon volcanic center is a buried peralkaline Miocene (13-15 m.y.) caldera structure located in southern Nye County about 40 km northeast of Beatty, Nev. (fig. 1). The caldera is slightly elliptical, having a northeast-southwest diameter of 27 km and a northwest-southeast diameter of about 19 km. At least five other volcanic centers of rhyodacitic to rhyolitic composition occur nearby (Ekren, 1968). Silent Canyon is probably the oldest of this group of centers, although the lavas and tuffs of the Salyer-Wahmonie center (Poole and others, 1965) may be of overlapping age.

Field and laboratory studies by the USGS (U.S. Geological Survey) completed during 1962-65 showed that the eastern part of Pahute Mesa was the probable source area for the Belted Range Tuff based on its thickness, distribution, and facies changes. Subsequent deep drilling and gravity data corroborated the location of the source of the Belted Range Tuff and provided information on the exact location, shape, structure, and evolution of the Silent Canyon center. Noble, Bath and others (1968) and Orkild, Byers and others (1968) showed that Silent Canyon activity commenced with the emplacement of tuffs, lava flows, domes, and dikes over an area of at least 1,165 km<sup>2</sup>. Most units were erupted from the general area of later caldera collapse but some vents marked by dikes, plugs, and flows, appear to occur along concentric-ring fracture zones outside the caldera boundary. One such zone of lavas lies 2-3 km outside the boundary, others are 8-13 km, and 21-22 km outside. Two compound cooling unit ash-flow sheets--the Tub Spring and overlying Grouse Canyon Members of the Belted Range Tuff--were then erupted. The Tub Spring had an estimated original volume of about 62.5-104 km<sup>3</sup> and covered an area of 2,590 km<sup>2</sup>. Collapse accompanying eruption was a minimum of 300 m on the Tub Spring caldera. The more voluminous Grouse Canyon covered 7,770 km<sup>2</sup> and had an original volume of about 208 km<sup>3</sup>. Collapse accompanying this eruption was 460-760 m. Tub Spring attains a thickness of 520 m within the caldera, with Grouse Canyon 540 m, while outside the caldera neither unit exceeds 120 m, and both are generally less than 60 m thick. The Belted Range Tuff was followed by extrusion of tuffs and lavas of Deadhorse Flat, lavas of Saucer Mesa, and the tuff of Basket Valley. The Deadhorse units occur inside the caldera along its north and east side. They reach a thickness of about 1,830 m. Saucer Mesa and Basket Valley flows occur outside the caldera to the north and east. They have a cumulative thickness of about 490 m and may in part be equivalent to the Deadhorse flows.

Although the main collapses were concomitant with extrusion of the Belted Range Tuff, additional collapse along the outermost caldera boundary must have accompanied extrusion of the later tuffs and lavas. Total vertical offset of 1,525-2,135 m within the caldera is known from drilling records.

#### Age of Silent Canyon Volcanic Center

Three dates were obtained on rocks of the Silent Canyon center. One of the youngest known flows, the rhyolite of Saucer Mesa was dated from a sample of nonhydrated glass by the  $Ar^{40}/K^{40}$  method at  $13.1 \pm 0.5$  m.y. Nonhydrated glass obtained from the Grouse Canyon Member of the Belted Range Tuff (near the middle of the volcanic pile) was dated by the same method at  $13.8 \pm 0.5$  m.y., and the rhyolite of Kawich Valley, the oldest known lava flow, was dated from sanidine by the  $Ar^{40}/K^{40}$  method at  $14.8 \pm 0.6$  m.y. (Noble, Sargent and others, 1968, p. 75).

#### Major-Element Geochemistry: Silent Canyon

One hundred and fifty-four chemical analyses have been determined for the rocks of the Silent Canyon volcanic center. About 80 percent are usable for this study, the others are highly altered with resulting aberrant values for one or more oxides. Of the usable analyses 12 are nonhydrated glasses, 12 are hydrated or partly hydrated, and the remainder are devitrified or crystalline. Nonhydrated glasses are believed to be best for analyses (Noble, 1970; Macdonald and Bailey, 1973) as secondary hydration, devitrification, and crystallization can affect sodium, potassium, fluorine, chlorine, magnesium, silica, and iron. For this reason the graphs accompanying this report identify those samples which are nonhydrated glasses, hydrated glasses, and those that are crystalline samples.

Representative samples of all the major volcanic units of the Silent Canyon center are provided. The Grouse Canyon and Tub Spring Members of the Belted Range Tuff, though not separately identified on the graphs, are especially well represented with 27 and 30 analyses, respectively. Likewise, the lavas are well represented. Of the 10 lava units, there are 2-14 analyses for each.

The Silent Canyon lavas and tuffs fall roughly into the lithologic category of either rhyolite or trachyte. The majority of these are peralkaline, that is, they have a molecular excess of  $Na_2O+K_2O$  over  $Al_2O_3$  (Macdonald, 1974). Such rocks are commonly characterized by high sodium-bearing pyriboles such as aegerine, aenigmatite, riebeckite, or arfvedsonite, and indeed, these may be seen in thin sections of many of the rocks. Plagioclase is generally absent, but if present is generally albite. The predominant feldspars are sodium-rich sanidine or anorthoclase. Within the peralkaline field the Silent Canyon rocks plot as comendites and a few comenditic trachytes. Comendites have relatively low iron and relatively high  $Al_2O_3$ . None plot as pantellerites (relatively high iron, low  $Al_2O_3$ ). Rocks from the center that are not peralkaline are broadly classified as subalkaline following the terminology of Noble and Christiansen (1974). The rocks are all oversaturated, the range of normative quartz being about 6 to 48 percent.  $SiO_2$  values (weight percent calculated water free) range from about 65 to nearly 80 percent. The trachytic lavas fall between 65 and 69 percent, trachytic soda rhyolites 69 to about 71 percent, but the bulk of comenditic lavas and tuffs fall between 74 and 77 percent silica. In general, the Silent Canyon rocks have about the

same  $\text{SiO}_2$  range as the rocks of the Timber Mountain caldera--located adjacent to the south--except there are no mafic equivalents for Silent Canyon rocks (compare Quinlivan and Byers, 1977). Silent Canyon rocks are lower in  $\text{Al}_2\text{O}_3$ ,  $\text{CaO}$ , and  $\text{MgO}$  and higher in total iron and alkalis than the Timber Mountain calc-alkaline volcanic rocks (Quinlivan and Byers, 1977).

The volcanic rocks of Silent Canyon span a near-continuous range of  $\text{SiO}_2$  contents of 65 to nearly 80 weight percent (figs. 2-5). Note however, the near absence of rocks with  $\text{SiO}_2$  contents of 67-70 weight percent and the abundance of analyzed rocks with 74-77 percent  $\text{SiO}_2$ . The rocks of Silent Canyon show near-linear variations of most major-element oxides with  $\text{SiO}_2$  (figs. 2-5). A plot of  $\text{K}_2\text{O}$  versus  $\text{SiO}_2$  (fig. 2) shows a relatively flat straight-line relationship dropping from about 5.8 percent  $\text{K}_2\text{O}$  at 65 percent  $\text{SiO}_2$  down to about 4.2 percent  $\text{K}_2\text{O}$  at 80 percent  $\text{SiO}_2$ . The same is true for the slope of  $\text{Na}_2\text{O}/\text{SiO}_2$  (fig. 2) except that its angle is steeper above about 76 percent  $\text{SiO}_2$ . The slope of the plot of total alkalis ( $\text{Na}_2\text{O}+\text{K}_2\text{O}$ ) versus  $\text{SiO}_2$  is similar to but slightly steeper than  $\text{Na}_2\text{O}/\text{SiO}_2$  from 65 to 76 percent  $\text{SiO}_2$ .  $\text{CaO}$ ,  $\text{MgO}$ , and  $\text{TiO}_2$  values (fig. 3) decrease continuously with respect to  $\text{SiO}_2$  from 65 to about 76 percent, then flatten or rise slightly from 76 to 80 percent  $\text{SiO}_2$ .

The  $\text{Al}_2\text{O}_3$  versus  $\text{SiO}_2$  plot (fig. 4) shows a continuous but not linear drop from an average high at the trachytic comendite end (65 percent  $\text{SiO}_2$ ) of about 16.4 percent  $\text{Al}_2\text{O}_3$  to about 10.4 percent  $\text{Al}_2\text{O}_3$  at 80 percent  $\text{SiO}_2$ . There may be a secondary trend in this plot at  $\text{SiO}_2$  of 74-76 percent. Here a slight separation of points may indicate high- and low-value  $\text{Al}_2\text{O}_3$  samples at 11.5-12.5 percent. Likewise, in the plot of total iron (as  $\text{FeO}$ ) versus silica (fig. 4) a split appears in the 74-76 percent silica interval. Two populations again appear; a higher iron trend, at about 3.4 percent, and a lower iron trend, about 2.4 percent  $\text{FeO}$ . Rocks in the higher iron group generally have a low phenocryst content (less than 10 percent phenocrysts), whereas the lower iron group has a high phenocrysts content (12-30 percent). This may reflect a slightly different magma chemistry from one point of extrusion to another, or it may reflect the evolving of two separate peralkaline magmas that overlap in time.

Other major-element variation diagrams of the Silent Canyon rocks include  $\text{Na}_2\text{O}+\text{K}_2\text{O}/\text{Al}_2\text{O}_3$  (calculated in molecular amounts) versus  $\text{SiO}_2$  (fig. 5). The first value is also known as the agpaite index (Macdonald, 1974). A line drawn at 1.0 separates the peralkaline rocks (above 1.0) from subalkaline rocks (below 1.0). If it were not for leaching of the alkalis ( $\text{Na}_2\text{O}$  and  $\text{K}_2\text{O}$ ), more rocks would plot above the 1.0 line. As can be seen here many hydrated glass and crystalline samples plot below the 1.0 line, whereas all nonhydrated glasses are above the 1.0 line. It is significant to note that many crystalline (or devitrified) samples yield values nearly as high as nonhydrated glasses. These samples are dense, relatively low-permeability rocks which apparently allowed little or no leaching of alkalis. Points plotted below 0.85 are rocks that are generally relatively porous and now altered. The trachytic and intermediate silica samples (65-71 percent  $\text{SiO}_2$ ) may have had alkalis leached from them. No nonhydrated glasses were analyzed from this group so we cannot determine if their alkali-alumina values were initially low. An anomalously high value at  $\text{SiO}_2$  65.5 percent (fig. 5) is caused by argillic alteration. Care must be taken in selection of field samples, but often even this is not enough to determine if the rock is altered.

In the plot of total iron as  $\text{FeO}$  versus normative quartz (fig. 6) we again see a separation of points into populations with high and low iron. This plot shows relatively flat trends at 3.4 and 2.4 percent  $\text{FeO}$  between 25 and 37 percent normative quartz.

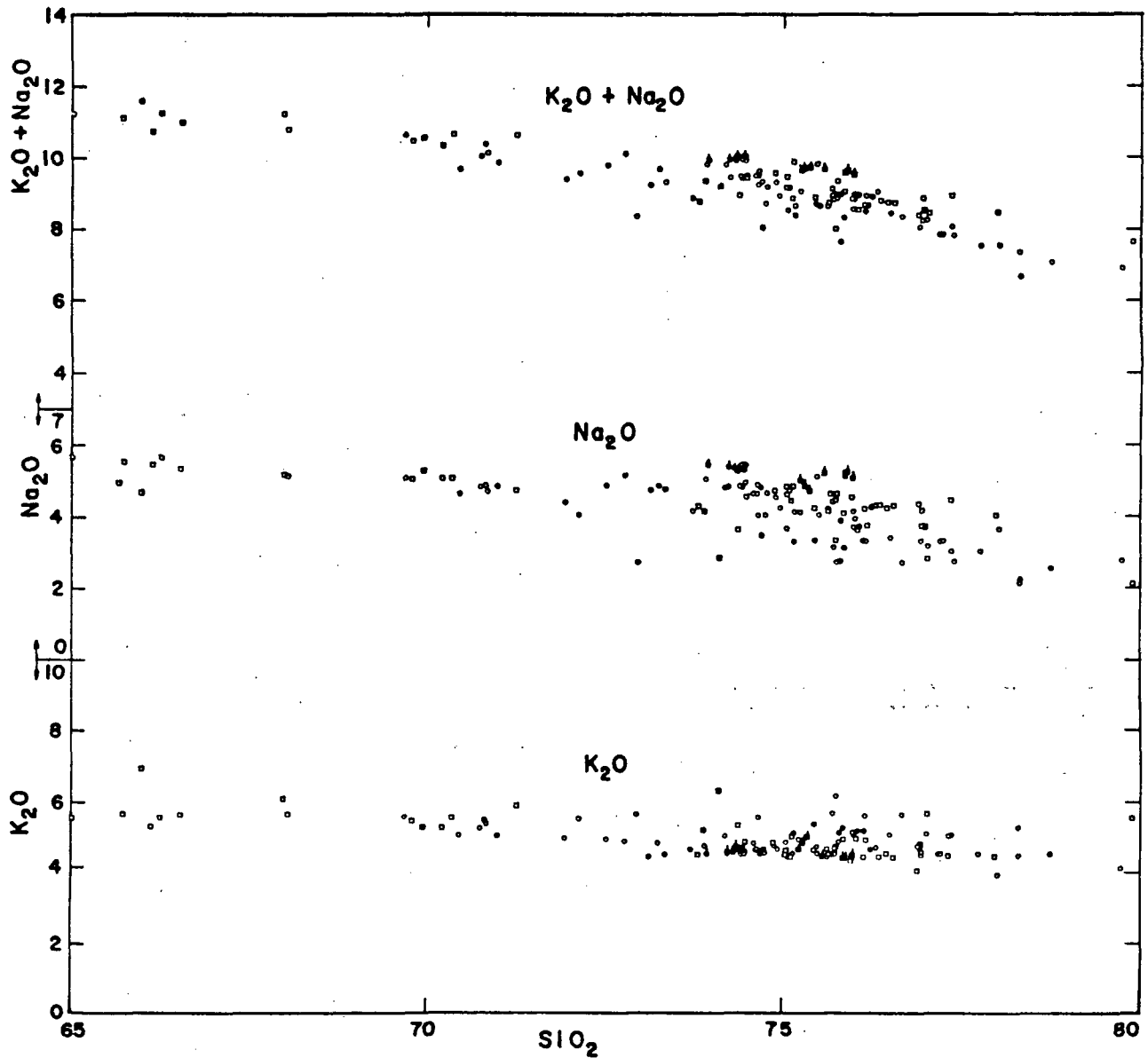


Figure 2.--Major-element oxide plots showing, respectively,  $\text{K}_2\text{O}$ ,  $\text{Na}_2\text{O}$ , and  $\text{K}_2\text{O} + \text{Na}_2\text{O}$  versus  $\text{SiO}_2$  for rocks of the Silent Canyon volcanic center.

Symbols:

- Analyzed sample from crystalline lava
- Analyzed sample from crystalline tuff
- and ● Analyzed sample of nonhydrated glass from lava (square) and tuff (circle)
- and ● Analyzed sample of hydrated glass from lava (square) and tuff (circle)

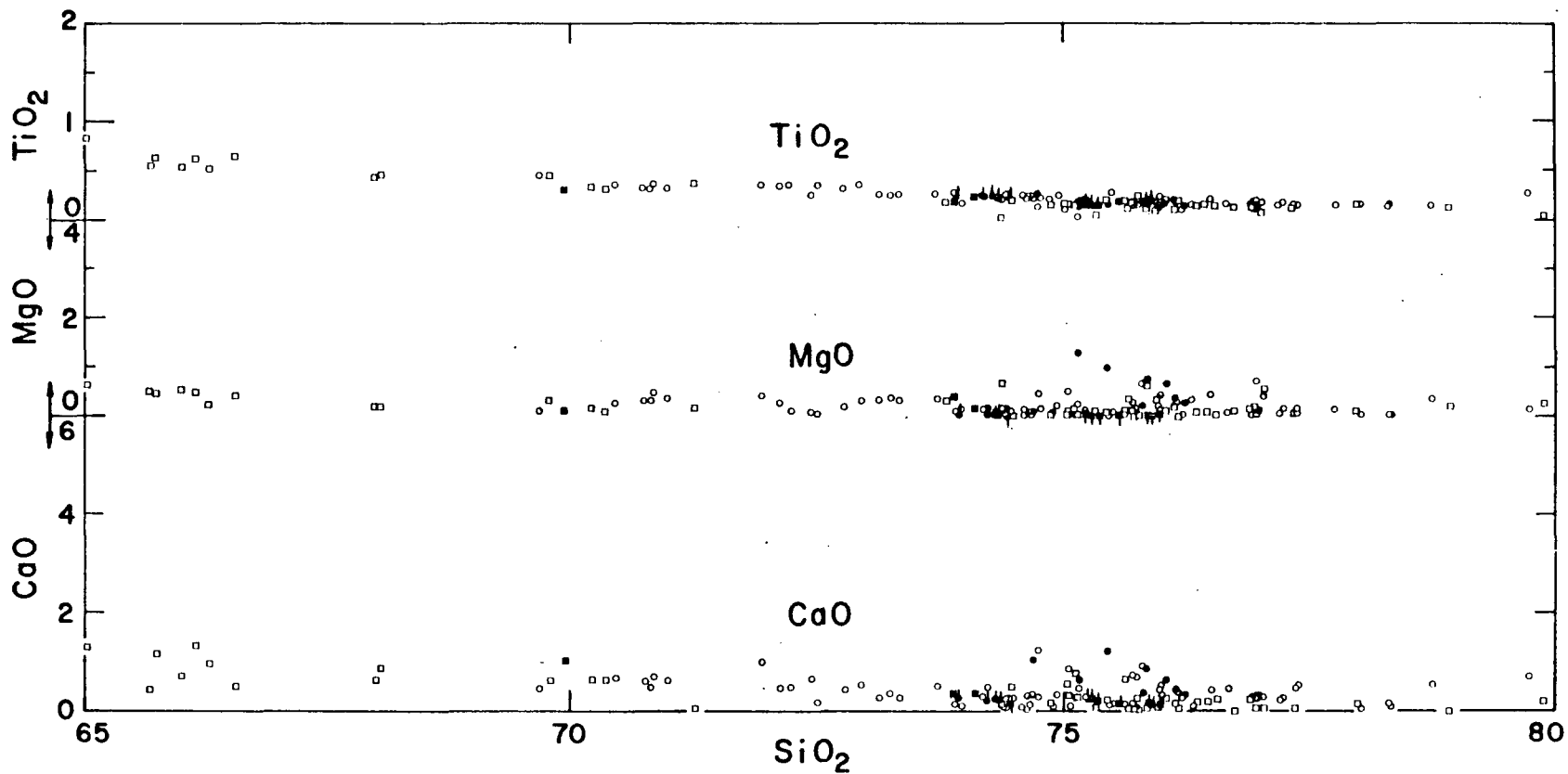


Figure 3.--Major-element oxide plots showing, respectively,  $\text{CaO}$ ,  $\text{MgO}$ , and  $\text{TiO}_2$  versus  $\text{SiO}_2$  for rocks of the Silent Canyon volcanic center.

Symbols:

- Analyzed sample from crystalline lava
- Analyzed sample from crystalline tuff
- and ● Analyzed sample of nonhydrated glass from lava (square) and tuff (circle)
- and ● Analyzed sample of hydrated glass from lava (square) and tuff (circle)

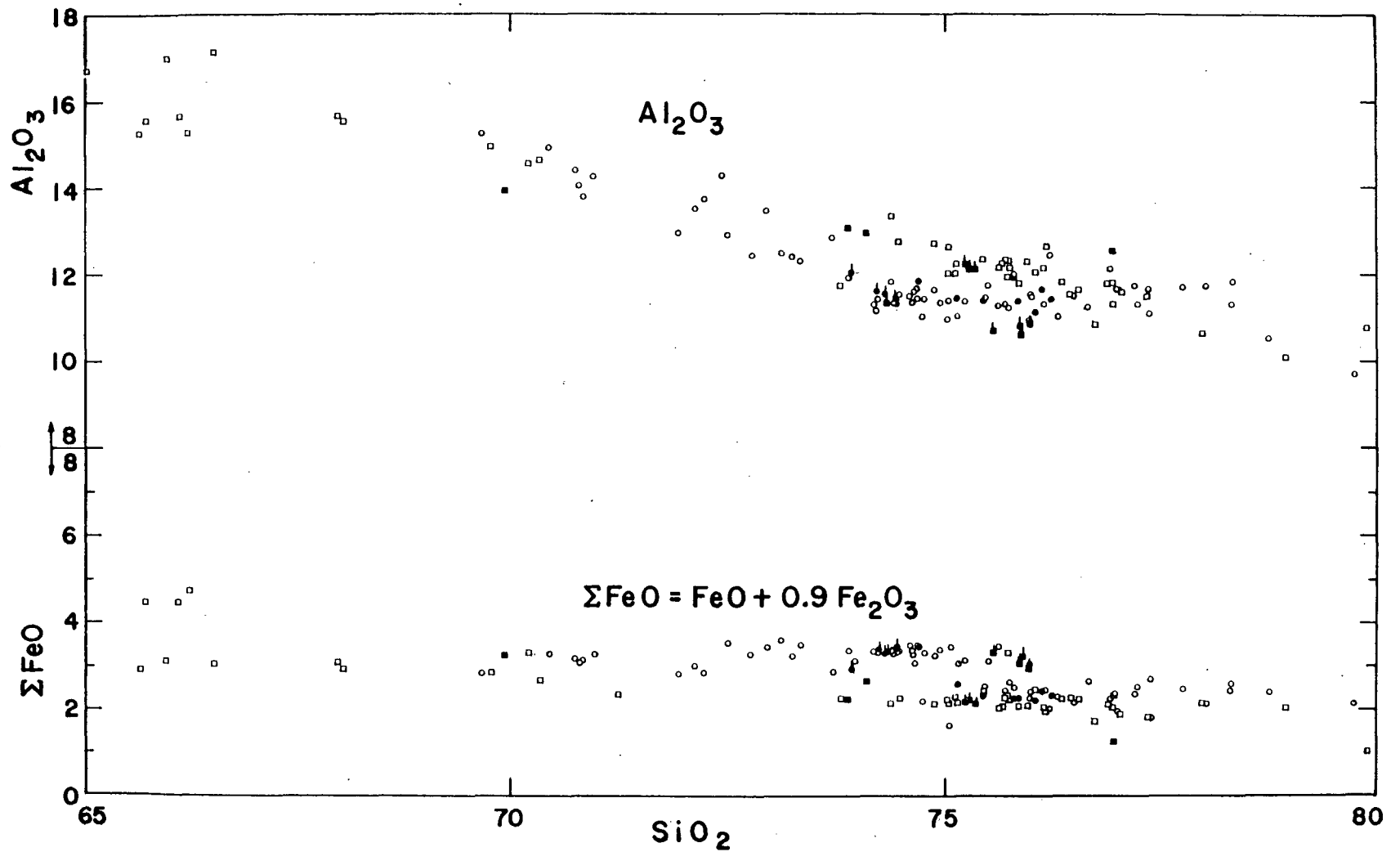


Figure 4.--Major-element oxide plots showing, respectively, total iron (as  $FeO + 0.9 Fe_2O_3$ ) and  $Al_2O_3$  versus  $SiO_2$  for rocks of the Silent Canyon volcanic center.

Symbols:

- Analyzed sample from crystalline lava
- Analyzed sample from crystalline tuff
- and ● Analyzed sample of nonhydrated glass from lava (square) and tuff (circle)
- ▣ and ● Analyzed sample of hydrated glass from lava (square) and tuff (circle)

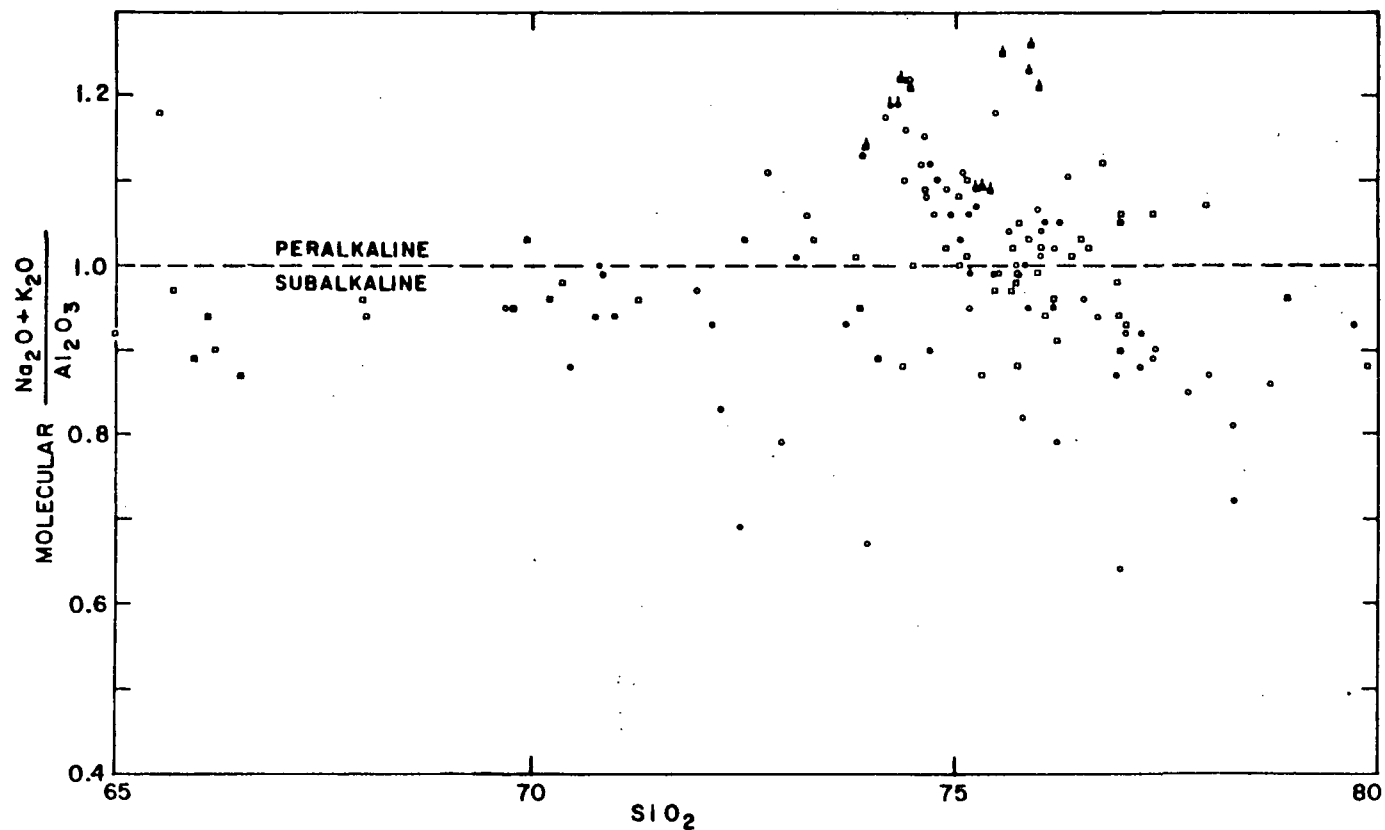


Figure 5.--Peralkalinity plot versus  $\text{SiO}_2$  for rocks of the Silent Canyon volcanic center. Peralkalinity defined by molecular  $\text{Na}_2\text{O}+\text{K}_2$  divided by  $\text{Al}_2\text{O}_3$ . Dashed line separates the peralkaline and subalkaline fields (molecular  $\text{Na}_2\text{O}+\text{K}_2=\text{Al}_2\text{O}_3$ ).

Symbols:

- Analyzed sample from crystalline lava
- Analyzed sample from crystalline tuff
- and ● Analyzed sample of nonhydrated glass from lava (square) and tuff (circle)
- and ● Analyzed sample of hydrated glass from lava (square) and tuff (circle)

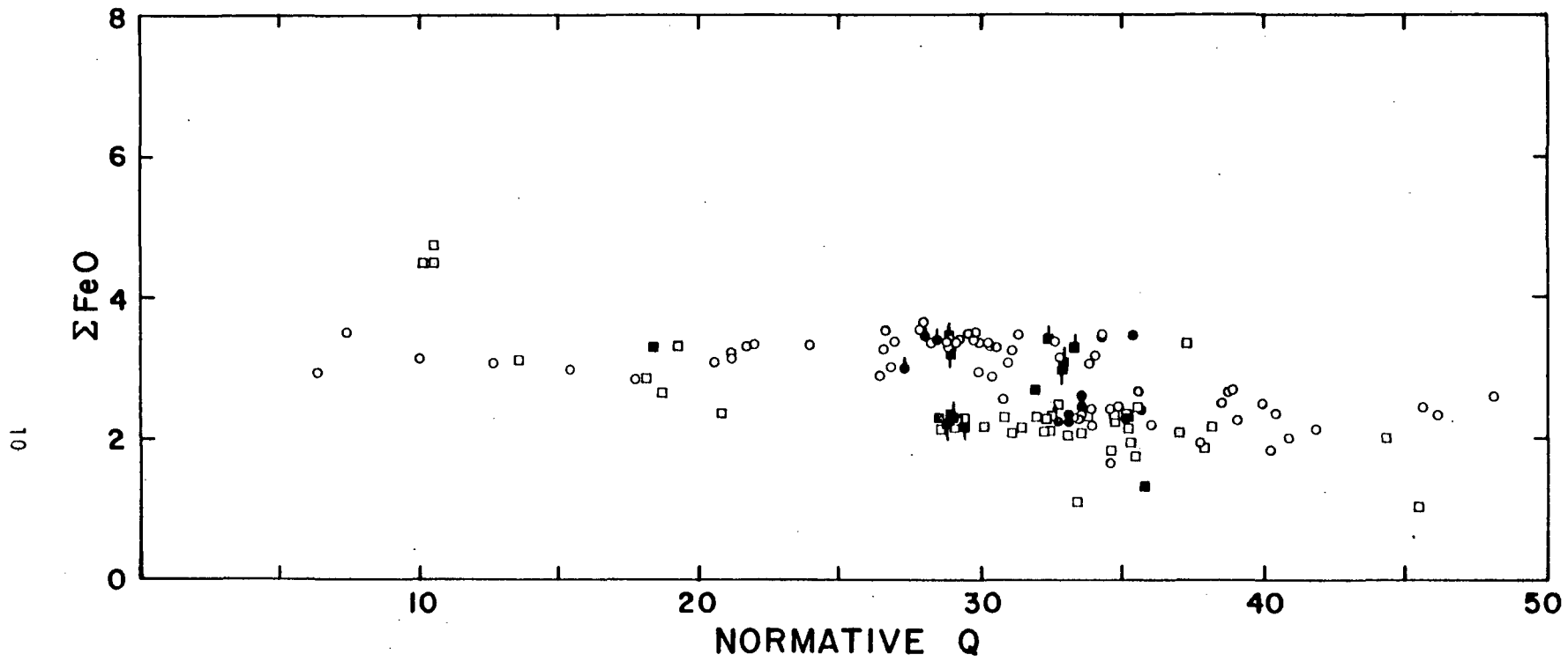


Figure 6.--Plot of total iron ( $FeO+0.9 Fe_2O_3$ ) versus normative quartz for rocks of the Silent Canyon volcanic center.

Symbols:

- $\square$  Analyzed sample from crystalline lava
- $\circ$  Analyzed sample from crystalline tuff
- $\blacksquare$  and  $\bullet$  Analyzed sample of nonhydrated glass from lava (square) and tuff (circle)
- $\blacksquare$  and  $\bullet$  Analyzed sample of hydrated glass from lava (square) and tuff (circle)

In a plot of  $Al_2O_3$  versus normative quartz (fig. 7), there is a consistent increase in normative quartz as  $Al_2O_3$  decreases in a nearly straight-line relationship. Nonhydrated glasses have lower values of normative quartz than units of equivalent  $Al_2O_3$  value suggesting that crystallization and hydration are related to an increase in  $SiO_2$ .

In summary, it appears that many crystalline and devitrified samples can be reliably used for plotting the rock chemistry. Samples need not be restricted to nonhydrated glasses although they are ideal if available. Hydrated glasses in many cases may be less reliable for analyses than crystalline samples. Crystalline samples should be as dense, nonporous, and impermeable as possible. Of the major oxides, sodium shows the greatest variation in values, presumably due to loss during cooling and subsequent alteration. Other oxides appear reliable except in samples with obvious deuteric, argillic, zeolitic, and ferrous alteration.

For the Silent Canyon rocks it appears from the plots that a slight change in magma chemistry due to either location, depth, or possibly pressure-temperature conditions have given rise to a chemical suite slightly higher in iron than the other. Consequently, those rocks constituting the high-iron suite do not fall on trend with other rocks of the center in all the plots. The high-iron rocks are primarily the Grouse Canyon Member of the Belted Range Tuff and the rhyolites of Split Ridge--both are poor in total percentage of phenocrysts. Other than being slightly higher in iron, and lower in alumina, they fall on trend with all the other rocks of the Silent Canyon volcanic center.

## BLACK MOUNTAIN VOLCANIC CENTER

### Geologic Setting and Evolution

Black Mountain volcanic center is an elliptical-shaped topographic depression located adjacent to and west of the Pahute Mesa that was the source for eruption of late Miocene lavas and voluminous ash-flow tuff (fig. 1). The volcanic center was mapped by Christiansen and Noble (1968) and Noble and Christiansen (1968). The center and associated volcanic rocks have been described by Noble and others (1964); Noble, Bath and others (1968); Christiansen and Noble (1965); Noble (1965); Ekren and others (1971); Noble and Christiansen (1974); and Noble and Parker (1974).

Volcanic rocks of the Black Mountain center have been divided into four cycles, each characterized by initial eruption of lavas followed by eruption of moderately voluminous ash-flow tuff. At least several and possibly all of the ash-flow cycles were succeeded by caldera collapse. Two major trends are shown by succeeding eruptive cycles: First, there was a progressive decrease in volume of eruptive products proceeding from the oldest to the youngest (Ekren and others, 1971). Second, the distribution of volcanic rocks of each cycle and particularly the progressive spatial restriction of younger cycle volcanic rocks to within preexisting caldera depressions suggests that successive cycles of activity were of decreased eruptive intensity than preceding cycles (R. L. Christiansen and D. C. Noble, written commun., 1974; Noble and Christiansen, 1968; Christiansen and Noble, 1968).

The following brief description of the evolution of Black Mountain volcanic center is modified largely from the written communication (1974) of R. L. Christiansen and D. C. Noble and from Ekren and others (1971). The oldest volcanic rocks of the Black Mountain center include a thick sequence of lava flows and thin pyroclastic deposits informally named the

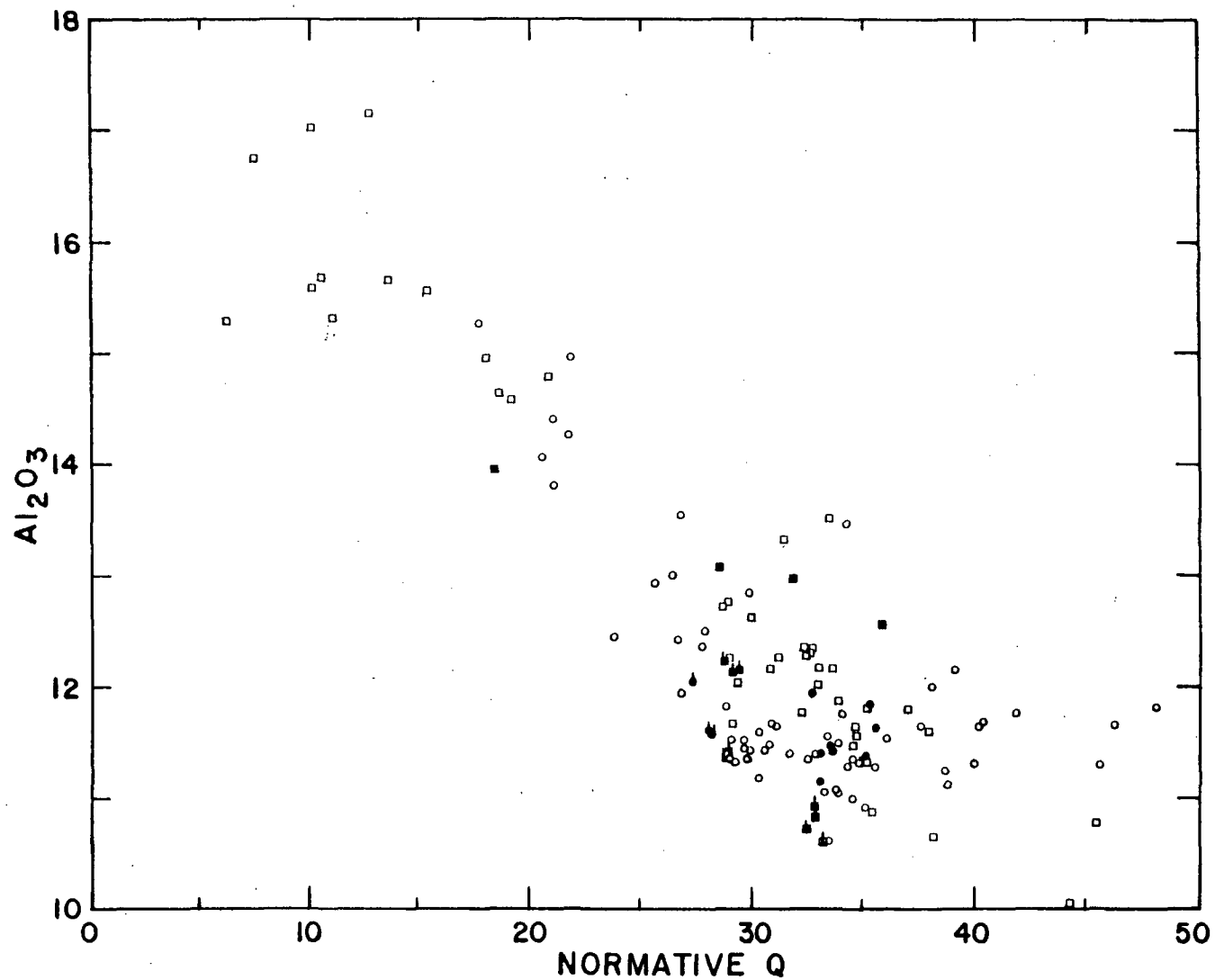


Figure 7.--Plot of Al<sub>2</sub>O<sub>3</sub> versus normative quartz for rocks of the Silent Canyon volcanic center.

Symbols:

□ Analyzed sample from crystalline lava

○ Analyzed sample from crystalline tuff

■ and ● Analyzed sample of nonhydrated glass from lava (square) and tuff (circle)

■ and ● Analyzed sample of hydrated glass from lava (square) and tuff (circle)

rhyolite of Ribbon Cliff. This unit, which ranges in composition from trachyte to trachytic soda rhyolite, occurs primarily within and to the east of the Black Mountain center. The rhyolite of Ribbon Cliff is overlain by ash-flow tuff of the Rocket Wash and Spearhead Members of the Thirsty Canyon Tuff which have an approximate volume of 20-25 km<sup>3</sup>. The eruption of the tuffs led to collapse of the volcanic center forming a caldera depression with an approximate diameter of 13 km. The two tuff units were originally mapped as a single unit, the Spearhead Member of the Thirsty Canyon Tuff (Noble and others, 1964). Subsequent fieldwork and paleomagnetic measurements (Noble, Bath and others, 1968) allowed recognition of two separate members (Rocket Wash and Spearhead Members) and suggested the possibility of caldera collapse following deposition of the Rocket Wash Member.

The second cycle of volcanic activity at Black Mountain was characterized by the development of a small lava volcano (trachyte of Yellow Cleft) within the Spearhead caldera depression. The throat of the volcano was intruded by a syenitic body that forms an arcuate-patterned intrusion exposed within the eastern half of the Spearhead caldera. The trachyte of Yellow Cleft is overlain by the Trail Ridge Member, an ash-flow tuff with similar distribution but smaller volume than the Rocket Wash and Spearhead Members. The eruptions of the Trail Ridge Member were followed by collapse that formed a small caldera probably contained within the Spearhead caldera. The third cycle of activity consisted of the eruption of the rhyolite of Pillar Spring. These lavas completely buried the Trail Ridge caldera but were contained within the larger Rocket Wash-Spearhead caldera. The rhyolite of Pillar Spring was succeeded by the Gold Flat Member (approximately 13 km<sup>3</sup>), a pantelleritic ash-flow tuff (Noble, 1965). The eruption of this unit led to the formation of a relatively small caldera depression with a diameter of approximately 6.5 km. The final cycle of salic activity of Black Mountain included eruption of the trachyte of Hidden Cliff which formed Black Mountain within the central part of the volcanic center. The constructional development of Black Mountain was followed by the eruption of the Labyrinth Canyon Member, a small volume ash-flow tuff that did not result in caldera collapse and was contained within the preexisting caldera depression. The youngest lavas apparently related to the Black Mountain volcanic center include the basalt of Basalt Ridge, a sequence of nepheline normative basalt flows which occur primarily northwest of Black Mountain.

#### Age of Black Mountain Volcanic Center

A number of K-Ar age determinations have been obtained for volcanic rocks of the Black Mountain center. The Rocket Wash and Labyrinth Canyon Members of the Thirsty Canyon Tuff have been dated at 7.5 and 6.2 m.y., respectively (Kistler, 1968). Armstrong, Dick, and Vitaliano (1972) have reported a date of 6.7 m.y. for the Spearhead Member. A fission-track date (zircon) of 8.2±0.9 m.y. was obtained for the syenite of Yellow Cleft (W. Carr, oral commun., 1978). The syenite of Yellow Cleft overlies the Spearhead Member and underlies the Trail Ridge Member of the Thirsty Canyon Tuff. Thus the fission-track date is older than and conflicts with the K-Ar age determinations. Additional and apparently conflicting whole-rock age determinations for the basalt of Basalt Ridge have been obtained of 10.3±0.9 m.y. (average of two analyses, W. Carr, oral commun., 1978). The basalt of Basalt Ridge overlies the Trail Ridge Member (Noble and Christiansen, 1968).

At present, the conflicting age determinations have not been resolved. Additional samples of the Thirsty Canyon Tuff will be dated.

#### Major-Element Geochemistry: Black Mountain

Thirty-four major-element chemical analyses of volcanic rocks of the Black Mountain center were obtained from published sources (Ekren and others, 1971; Noble, Bath and others, 1968; Noble and Christiansen, 1974; Noble and Parker, 1974) and from the data files of the USGS. The analyses provide a relatively complete representation of the major-element geochemistry for the various stratigraphic units of Black Mountain center with the exception of the trachyte of Yellow Cleft (one analysis) and the Labyrinth Canyon Member (one analysis). Chemical data from several of the published sources are averages of multiple analyses. Additionally, there is limited stratigraphic control on sample locations of specimens collected from the various stratigraphic units. Consequently, the geochemical data were examined only to evaluate the major-element chemical characteristics of the suite.

The lavas and tuffs of Black Mountain comprise a subalkaline-peralkaline association (Noble and Christiansen, 1974). The rocks are all oversaturated (quartz normative) with the exception of the basalt of Basalt Ridge (nepheline normative). Normative quartz ranges in weight percent from about 5 to 15 percent for the trachyte and trachytic rhyolites of the lava sequences (one analysis, the trachyte of Hidden Cliff just crosses the  $\text{SiO}_2$ -saturation boundary with 0.3 weight percent normative quartz) to about 22-30 percent for the trachytic soda rhyolites and comendites of the ash-flow sequences.  $\text{SiO}_2$  values (weight percent calculated water free) range from about 55 to 75.5 percent; the bulk of the analyzed rocks fall in the range of 65 to 75 percent  $\text{SiO}_2$ . In general, lavas tend to be relatively silica poor (trachytes and trachytic rhyolites) and the ash-flows more silica rich (trachytic rhyolites and comendites).

Major-element oxides versus silica are plotted for volcanic rocks of the Black Mountain center on figures 8-13. In general, the Black Mountain rocks are lower in  $\text{SiO}_2$ ,  $\text{Al}_2\text{O}_3$ ,  $\text{CaO}$ , and  $\text{MgO}$  and higher in total iron and alkalis than typical calc-alkaline volcanic rocks (compare with, for example, the calc-alkaline and alkalic-calcic volcanic rocks of the Timber Mountain-Oasis Valley caldera complex; Quinlivan and Byers, 1977; Christiansen and others, 1977).

Figures 8-10 include plots of major-element oxides versus  $\text{SiO}_2$ . Rocks of the Black Mountain center span a  $\text{SiO}_2$  range of 55 to 75 weight percent. Note however, the conspicuous absence of rocks with  $\text{SiO}_2$  contents between 55 and 60 percent and the less prominent gap between 64 and 66 percent. At present it is not known whether these gaps are real or reflect data bias introduced by the limited number of available chemical analyses. The volcanic rocks of Black Mountain show slight-curving linear variations of most major-element oxides with  $\text{SiO}_2$  (fig. 8-10).  $\text{K}_2\text{O}/\text{SiO}_2$  plots show a relatively smooth curve with maximum  $\text{K}_2\text{O}$  values occurring in the range of 66 to 67 percent  $\text{SiO}_2$ ;  $\text{Na}_2\text{O}/\text{SiO}_2$  plots exhibit a relatively flat curve (slope near 0) with  $\text{Na}_2\text{O}$  values falling largely between 4.0 and 6.0 weight percent through the range of  $\text{SiO}_2$  contents; total alkalis versus  $\text{SiO}_2$  show a relatively smooth curve with average alkali values of about 10.0 weight percent and reaching a maximum of slightly greater than 11.0 percent for rocks falling in the range of 66 to 69 percent  $\text{SiO}_2$  (fig. 8).  $\text{CaO}$  values decline continuously with increasing  $\text{SiO}_2$  from a maximum value of 6.0 percent at 55 percent  $\text{SiO}_2$ ; likewise,  $\text{MgO}$  values decline from slightly greater than 3.0 percent for the trachyte of Hidden Cliff to

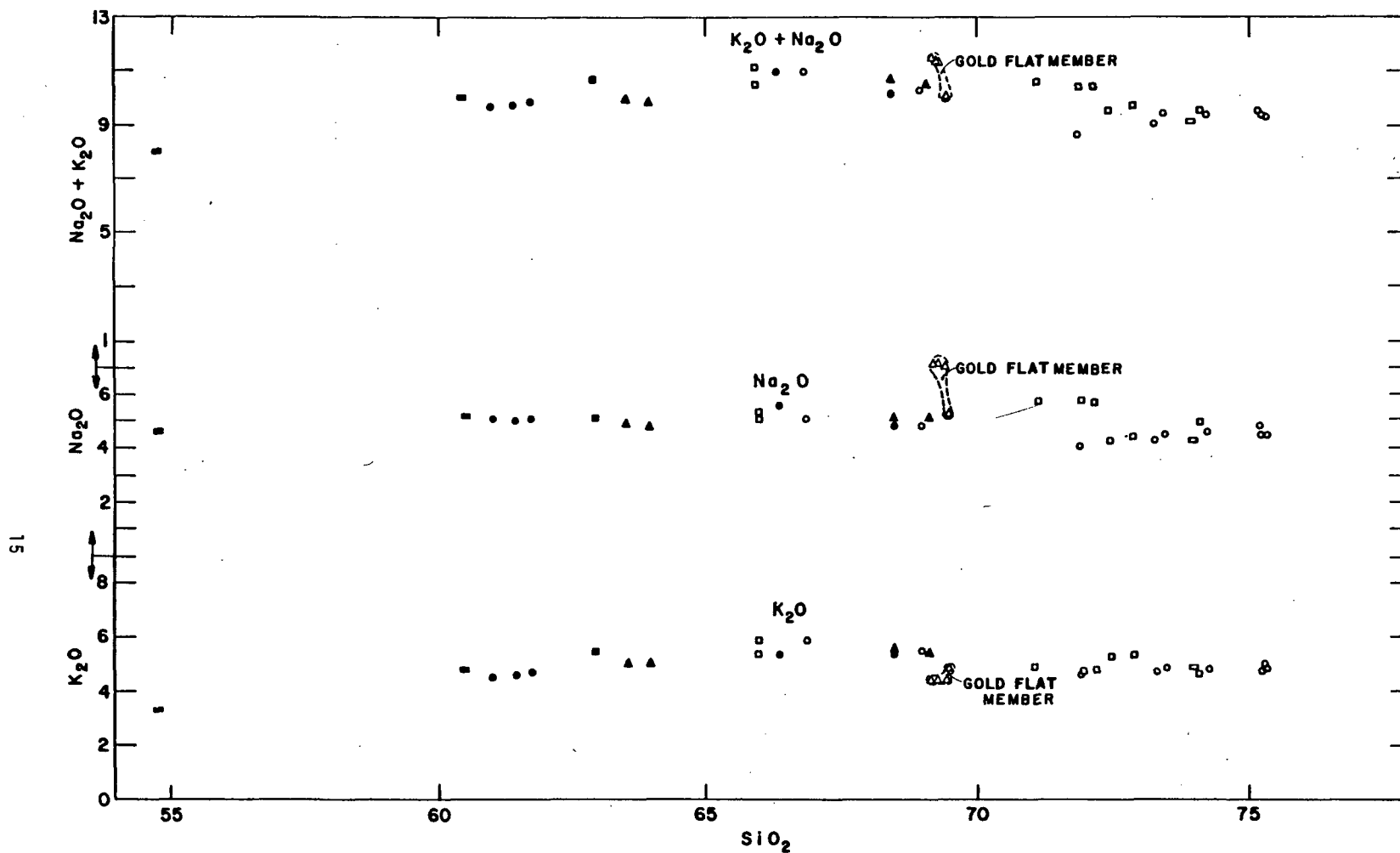


Figure 8.--Major-element oxide plots showing, respectively,  $\text{K}_2\text{O}$ ,  $\text{Na}_2\text{O}$ , and  $\text{K}_2\text{O}+\text{Na}_2\text{O}$  versus  $\text{SiO}_2$  for rocks of the Black Mountain volcanic center.

Symbols:

- Lavas of Ribbon Cliff
- Rocket Wash and Spearhead Members of Thirsty Canyon Tuff
- Syenite of Yellow Cleft
- Trailridge Member of Thirsty Canyon Tuff
- ▲ Lavas of Pillar Spring
- △ Gold Flat Member of Thirsty Canyon Tuff
- Trachyte of Hidden Cliff
- Labyrinth Canyon Member of Thirsty Canyon Tuff

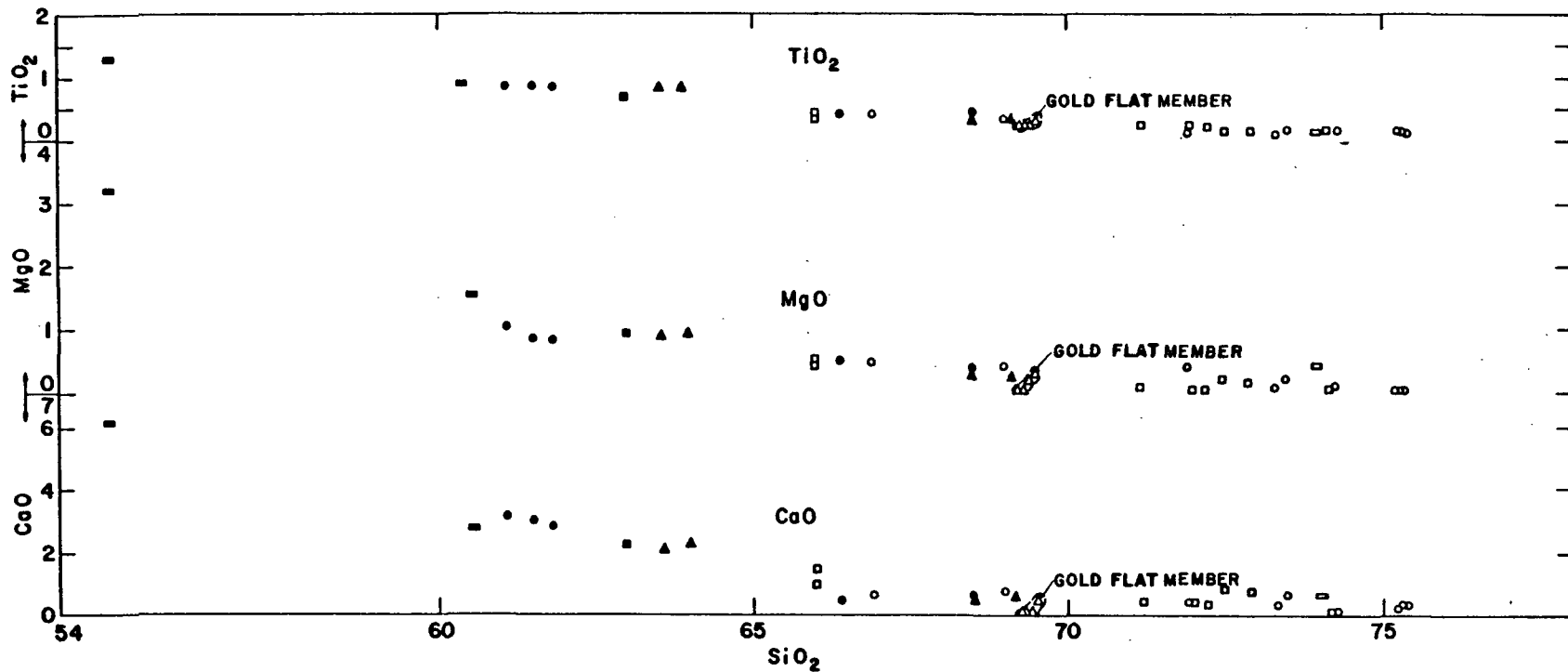


Figure 9.--Major-element oxide plots showing, respectively, CaO, MgO, and TiO<sub>2</sub> versus SiO<sub>2</sub> for rocks of the Black Mountain volcanic center.

Symbols:

- Lavas of Ribbon Cliff
- Rocket Wash and Spearhead Members of Thirsty Canyon Tuff
- Syenite of Yellow Cleft
- Trailridge Member of Thirsty Canyon Tuff
- ▲ Lavas of Pillar Spring
- △ Gold Flat Member of Thirsty Canyon Tuff
- Trachyte of Hidden Cliff
- Labyrinth Canyon Member of Thirsty Canyon Tuff

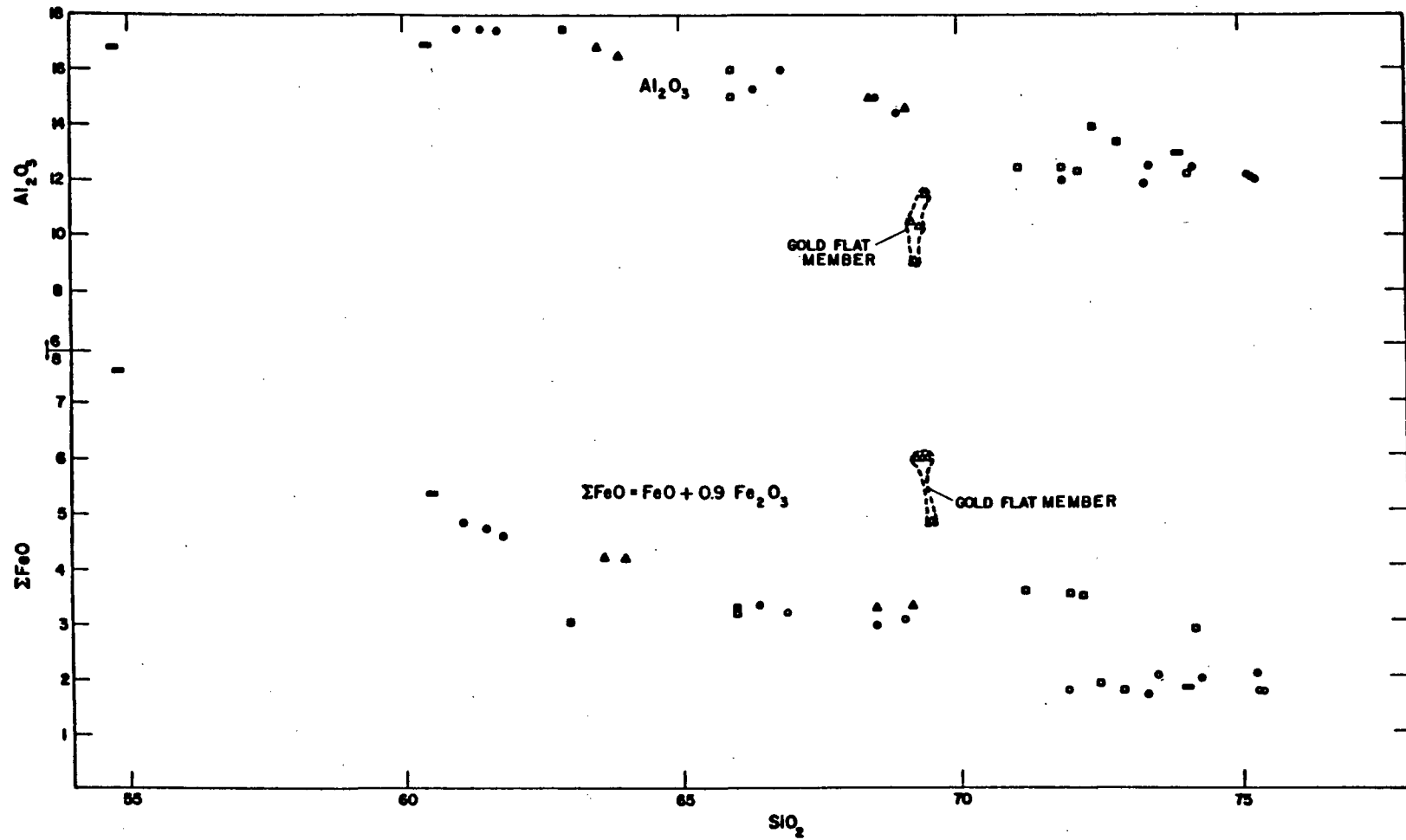


Figure 10.--Major-element oxide plots showing, respectively, total iron (as  $\text{FeO} + 0.9 \text{Fe}_2\text{O}_3$ ) and  $\text{Al}_2\text{O}_3$  versus  $\text{SiO}_2$  for rocks of the Black Mountain volcanic center.

Symbols:

- Lavas of Ribbon Cliff
- Rocket Wash and Spearhead Members of Thirsty Canyon Tuff
- Syenite of Yellow Cleft
- Trailridge Member of Thirsty Canyon Tuff
- ▲ Lavas of Pillar Spring
- △ Gold Flat Member of Thirsty Canyon Tuff
- Trachyte of Hidden Cliff
- Labyrinth Canyon Member of Thirsty Canyon Tuff

generally less than 0.5 percent for the higher SiO<sub>2</sub> rocks (fig. 9). TiO<sub>2</sub> values decline from 1.3 weight percent for the trachyte of Hidden Cliff to less than 0.2 weight percent for the trachytic soda rhyolites and comendites.

Several major-element oxide plots exhibit slightly to markedly divergent trends that are consistent for the respective plots. These trends are well shown by the Al<sub>2</sub>O<sub>3</sub>/SiO<sub>2</sub> plot (fig. 10). First, Al<sub>2</sub>O<sub>3</sub> values are generally higher for the trachytic rocks (16-18 percent) and decline markedly for the more silica-rich rocks. Second, Al<sub>2</sub>O<sub>3</sub> values for the pantelleritic Gold Flat Member of the Thirsty Canyon Tuff are distinctly lower (9-11 weight percent) than other rocks of the Black Mountain center. Third, there is a slight divergence in Al<sub>2</sub>O<sub>3</sub> values within the most SiO<sub>2</sub>-rich rocks of the center. This is perhaps most noticeable for the Trail Ridge Member of the Thirsty Canyon Tuff. Oxide plots of total iron (as FeO) versus SiO<sub>2</sub> and Na<sub>2</sub>O/SiO<sub>2</sub> likewise show somewhat divergent trends and support the trends noted for the Al<sub>2</sub>O<sub>3</sub>/SiO<sub>2</sub> diagram. Note on both the FeO/SiO<sub>2</sub> diagram (fig. 10) and the Na<sub>2</sub>O/SiO<sub>2</sub> diagram (fig. 8), the divergent positions of plots of the Gold Flat Member of the Thirsty Canyon Tuff and the scatter and apparent separation for plots within the more SiO<sub>2</sub>-rich rocks.

Three additional plots serve to further characterize the geochemical character of the Black Mountain volcanic center. Figure 11 is a plot of atomic Na+K divided by Al versus SiO<sub>2</sub> with the peralkaline-subalkaline boundary shown by a dashed line (atomic Na+K equal to atomic Al<sup>1</sup>). The Black Mountain volcanic rocks exhibit a marked increase in peralkalinity with increasing SiO<sub>2</sub>. In general, rocks in the compositional range of trachyte are of subalkaline composition and more silicic rocks plot along and overlap the peralkaline boundary (rhyolites to comendites). This increase in peralkalinity with increasing SiO<sub>2</sub> is similar to geochemical trends indicated by the volcanic rocks of the Trans-Pecos volcanic province (see Barker, 1977, fig. 3). Two additional points are significant for this diagram: (1) the extreme peralkaline compositions of the pantelleritic Gold Flat Member and (2) the separation of the Trail Ridge plots into peralkaline (comendites) and subalkaline compositions. Figure 12 is a plot of total iron as FeO versus normative quartz. This diagram illustrates the aberrant chemical character of the rocks of the Gold Flat Member and the scatter in total iron contents of rocks of the Trail Ridge Member. The same features are additionally shown on figure 13, a plot of Al<sub>2</sub>O<sub>3</sub> versus normative quartz. Again note the divergent position of the plots of the Gold Flat Member and the scatter within plots of the Trail Ridge Member.

#### GEOCHEMICAL COMPARISON: BLACK MOUNTAIN-SILENT CANYON CENTERS

Volcanic rocks of the Black Mountain and Silent Canyon centers are broadly similar geochemically. Both suites include subalkaline and peralkaline rocks with the bulk of silica-rich rocks falling into the compositional categories of comendites and comenditic trachytes (classification of Macdonald, 1974). The suites exhibit largely similar variations of K<sub>2</sub>O and Na<sub>2</sub>O with respect to SiO<sub>2</sub> (figs. 2, 8). CaO, MgO, and TiO<sub>2</sub> values are similar although higher values for the respective oxide contents are reached in the more mafic rocks of the Black Mountain center (figs. 3, 9).

---

<sup>1</sup>Peralkalinity values were calculated using molecular percent for the Silent Canyon volcanic rocks and atomic percent for the Black Mountain volcanic rocks. The two calculation procedures are identical within the limits of precision of the analytical techniques used to obtain the chemical data.

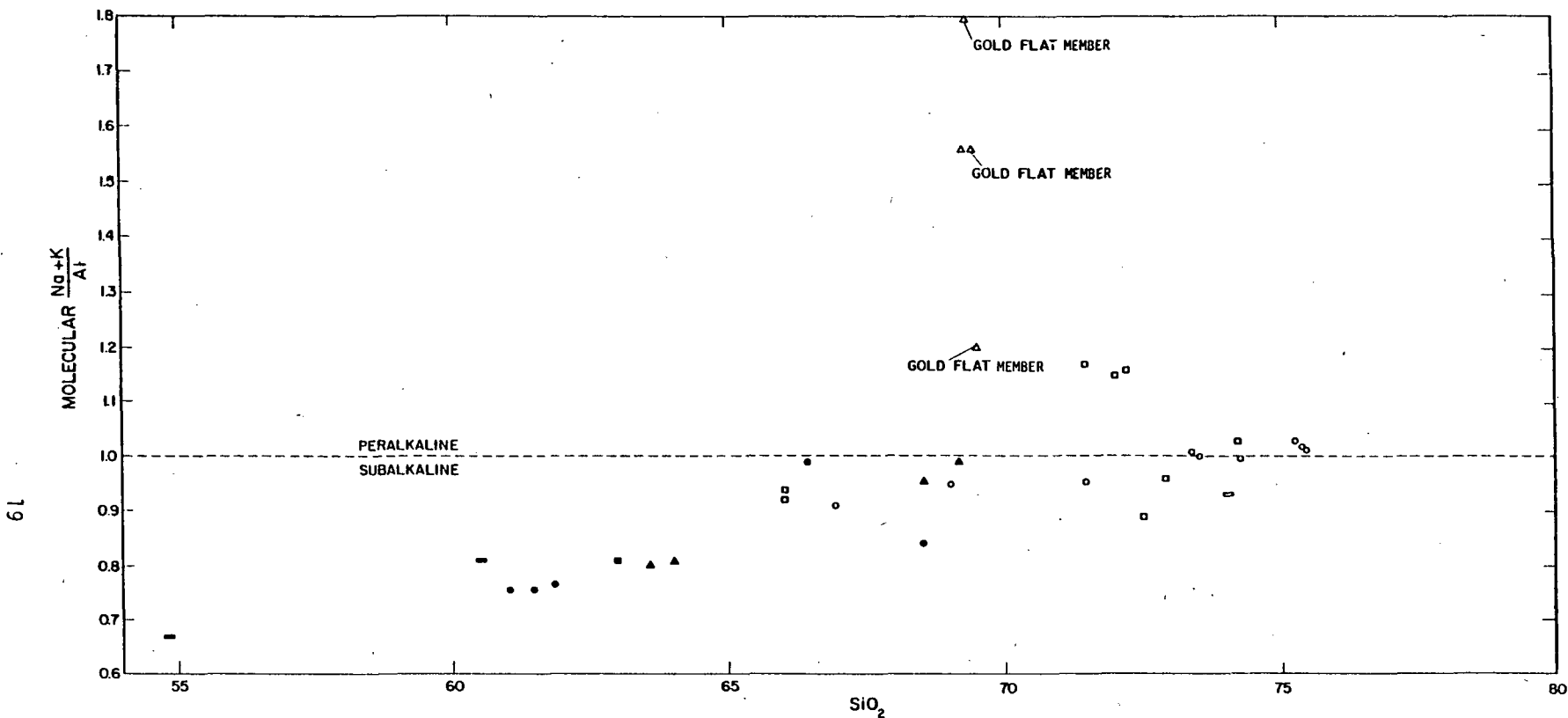


Figure 11.--Peralkalinity plot versus  $\text{SiO}_2$  for rocks of the Black Mountain volcanic center. Peralkalinity defined by atomic  $\text{Na}+\text{K}$  divided by  $\text{Al}$ . Dashed line separates the peralkaline and subalkaline fields (atomic  $\text{Na}+\text{K}=\text{Al}$ ).

Symbols:

- Lavas of Ribbon Cliff
- Rocket Wash and Spearhead Members of Thirsty Canyon Tuff
- Syenite of Yellow Cleft
- Trailridge Member of Thirsty Canyon Tuff
- ▲ Lavas of Pillar Spring
- △ Gold Flat Member of Thirsty Canyon Tuff
- ▬ Trachyte of Hidden Cliff
- Labyrinth Canyon Member of Thirsty Canyon Tuff

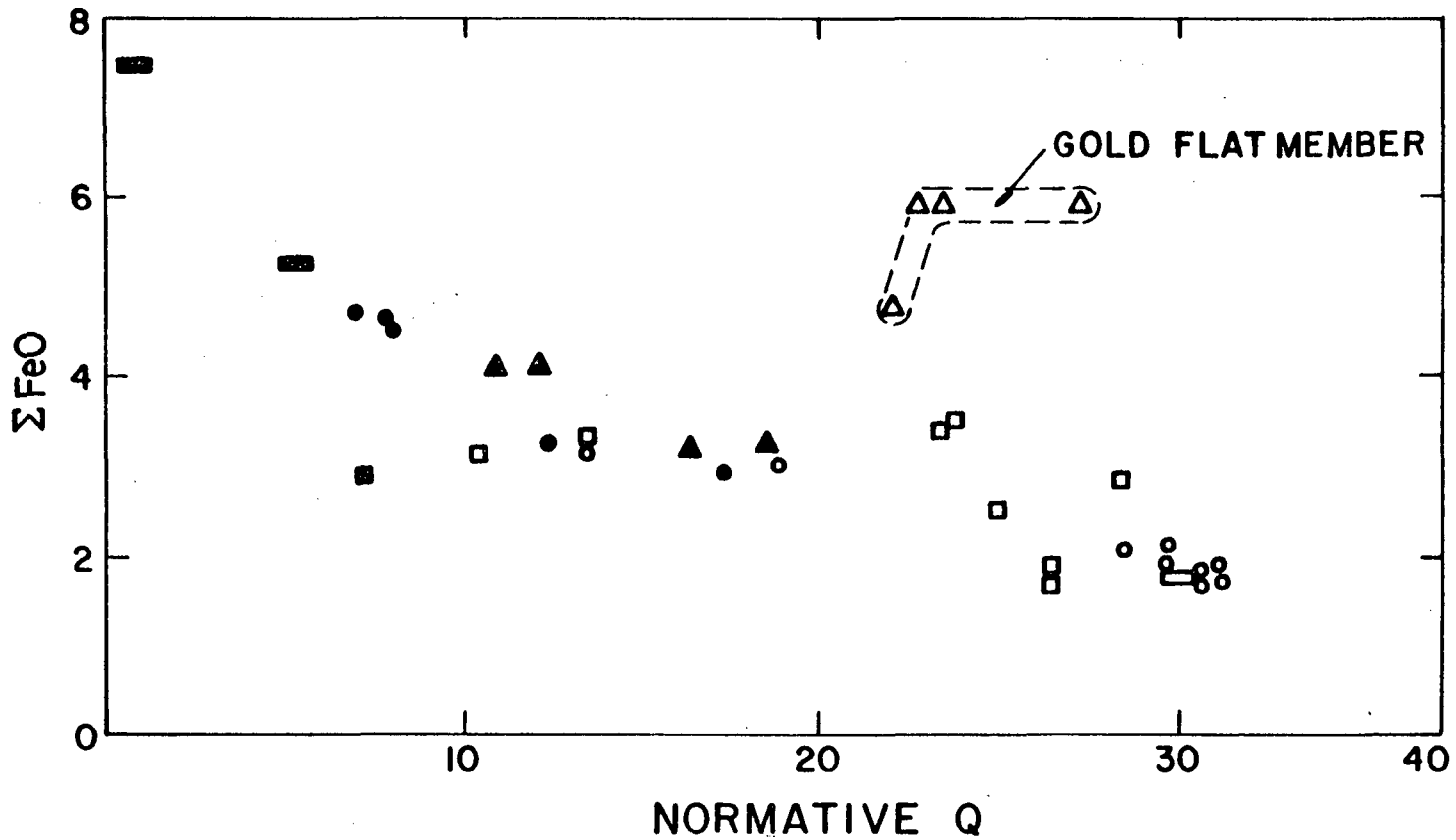


Figure 12.--Plot of total iron ( $\text{FeO} + 0.9 \text{Fe}_2\text{O}_3$ ) versus normative quartz for rocks of the Black Mountain volcanic center.

Symbols:

- Lavas of Ribbon Cliff
- Rocket Wash and Spearhead Members of Thirsty Canyon Tuff
- Syenite of Yellow Cleft
- Trailridge Member of Thirsty Canyon Tuff
- ▲ Lavas of Pillar Spring
- △ Gold Flat Member of Thirsty Canyon Tuff
- Trachyte of Hidden Cliff
- Labyrinth Canyon Member of Thirsty Canyon Tuff

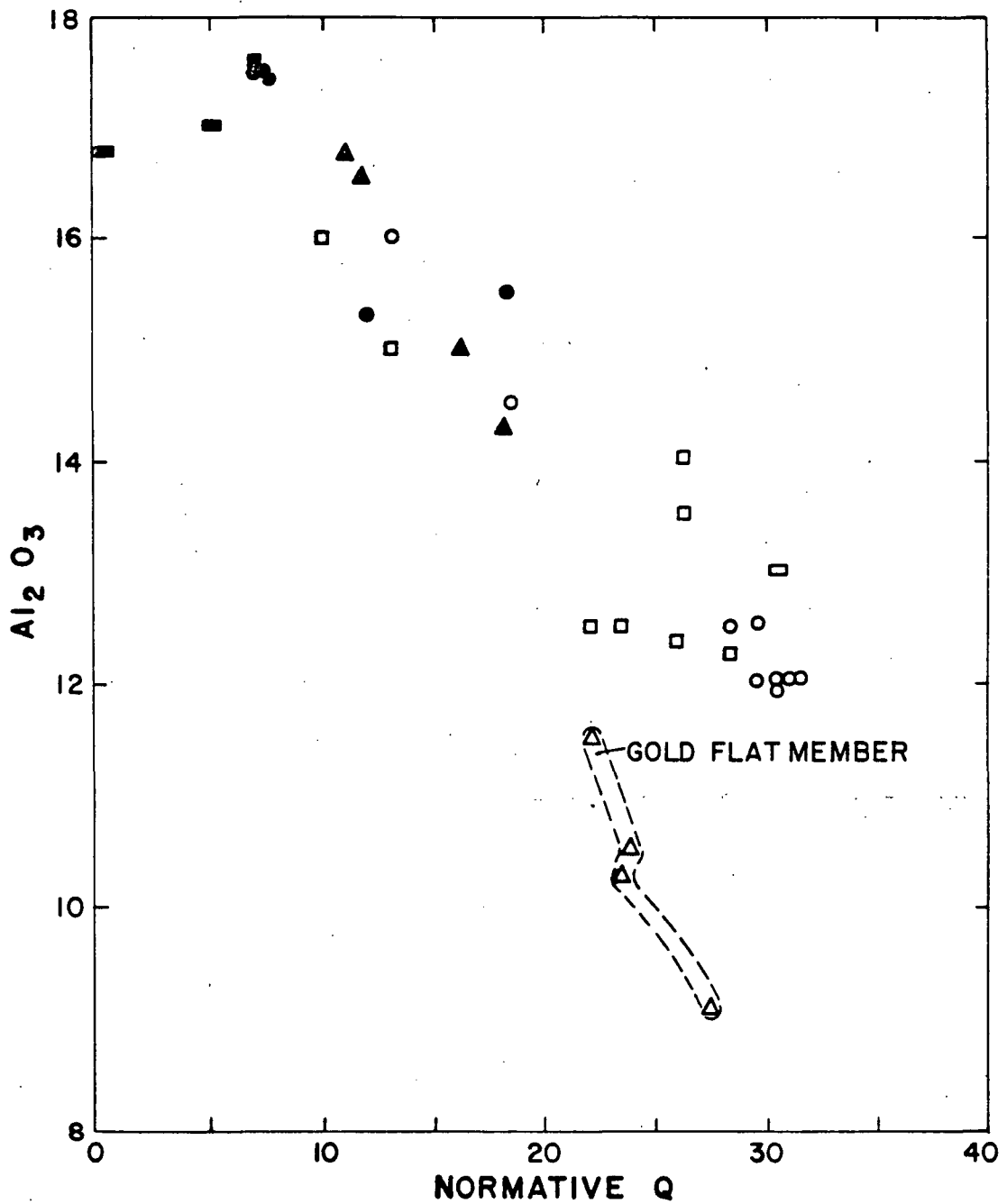


Figure 13.--Plot of Al<sub>2</sub>O<sub>3</sub> versus normative quartz for rocks of the Black Mountain volcanic center.

Symbols:

- Lavas of Ribbon Cliff
- Rocket Wash and Spearhead Members of Thirsty Canyon Tuff
- Syenite of Yellow Cleft
- Trailridge Member of Thirsty Canyon Tuff
- ▲ Lavas of Pillar Spring
- △ Gold Flat Member of Thirsty Canyon Tuff
- Trachyte of Hidden Cliff
- Labyrinth Canyon Member of Thirsty Canyon Tuff

In detail, however, the suites differ in several ways. The total range and distribution of  $\text{SiO}_2$  contents for rocks of the respective centers are strikingly different. The majority of analyzed rocks of the Silent Canyon center have  $\text{SiO}_2$  contents ranging from 73 to 80 weight percent; the most mafic of the analyzed rocks have  $\text{SiO}_2$  contents of 65 percent. In contrast, rocks of the Black Mountain center have  $\text{SiO}_2$  values as low as 55 percent and the majority of the comenditic ash-flow tuffs have  $\text{SiO}_2$  values of 74-77 weight percent. Rocks of the Silent Canyon center plot largely along and closely adjacent to the peralkaline-subalkaline boundary (fig. 5); the Black Mountain volcanic rocks trend sharply across this boundary and the trachytic rocks fall well below the subalkaline-peralkaline boundary (fig. 11). The Black Mountain volcanic rocks include the pantelleritic Gold Flat Member, a strongly peralkaline ash-flow tuff. This unit is both richer in iron and more deficient in alumina than any rocks of the Silent Canyon center. Plots of total iron versus normative quartz for volcanic rocks of the Black Mountain and Silent Canyon centers (figs. 6, 12, respectively) illustrate two major differences between the suites: (1) the higher maximum values of normative quartz for the Silent Canyon rocks, reflecting the higher  $\text{SiO}_2$  contents, (2) the slight tendency toward greater FeO contents for the higher normative quartz values of the Silent Canyon center, except for the high FeO contents of the Gold Flat Member. Note particularly the near-flat trend of the FeO versus normative quartz curve for Silent Canyon in contrast to the sharp decrease in FeO with normative quartz for Black Mountain volcanic rocks.

All the geochemical differences discussed above strongly suggest that the rocks of the Black Mountain and Silent Canyon volcanic centers were unrelated and evolved from differing magma bodies. The tectonic setting and ultimate origin of these rocks may have been related, however each evolved with no overlap in time and little, if any, overlap in space.

#### Volcanic Hazards: Nevada Nuclear Waste Storage Investigations

Major-element geochemical comparisons of the Silent Canyon-Black Mountain volcanic centers indicate they represent spatially and temporally distinct episodes of volcanic activity. This is supported by two lines of evidence. Geologic mapping and drill-hole data indicate that there is no overlap of the Black Mountain and Silent Canyon volcanic centers (Orkild and others, 1969). Although widely distributed ash-flow sheets of the centers overlap, there is no overlap of volcanic source vents. This strongly suggests that the respective centers are spatially separate. The rocks of the Black Mountain center stratigraphically overlie and are therefore younger than those of the Silent Canyon center. The two sequences are separated stratigraphically by the tuffs of Area 20, the Paintbrush and Timber Mountain Tuffs and post-Timber Mountain tuffs and rhyolite of the Timber Mountain caldera cycle (Orkild and others, 1969; Byers and others, 1976). These intervening sequences have K-Ar ages ranging from 13.1 to 9.5 m.y. (Kistler, 1968). The age range of volcanic activity at Black Mountain volcanic center, however, has not been completely resolved by K-Ar dating. Available age dates (Kistler, 1968; Armstrong and others, 1972) for the volcanic centers suggest Black Mountain center is distinctly younger than the Silent Canyon center and that the magnitude of the age gap between the centers exceeds the range of analytical uncertainty of the K-Ar age determinations. Finally, examination of the major-element chemical characteristics of the volcanic centers reveal differences that suggest the respective lavas evolved from chemically distinct magma bodies.

The above data indicate that Black Mountain volcanism represents a distinct episode of eruptive activity. Consequently, it represents a separate and renewed phase of volcanism following a relatively brief magmatic hiatus. Moreover, the activity of Black Mountain was relatively large volume and highly explosive--factors that increase the disruptive potential of volcanic activity.

Several lines of evidence suggest that the magmatic cycle of activity of Black Mountain is complete. First, the youngest volcanic rocks of the center are probably on the order of 7 m.y. old. Cooling times for large silicic bodies, assuming heat loss by conduction, are probably less than 2 m.y. unless the heat has been replenished by new magma injected at depth (Lachenbruch and others, 1976; Kolstad and McGetchin, 1978). This suggests that the magma body that fed Black Mountain volcanism is probably completely solidified. Second, the volume of volcanic material erupted during successive cycles of activity declined progressively. This suggests a systematic waning of volcanism consistent with the cessation of volcanism being marked by the youngest activity (basalt of Basalt Ridge or the Labyrinth Canyon Member).

There remains a finite but numerically incalculable probability of recurrence of Black Mountain-type volcanism within the NTS region. This possibility needs to be considered in an evaluation of long-term risk associated with geologic isolation of radioactive waste at the NTS. Qualitatively the risk of recurrence of Black Mountain-type volcanism is probably small. However, any type of quantitative evaluation of risk is beyond the present state of geologic knowledge concerning Great Basin volcanism. Several additional types of data would be beneficial for a continued evaluation of volcanic risk. First, the geochemical data for the Black Mountain and Silent Canyon volcanic centers need to be contrasted with existing geochemical data for peralkaline volcanism and post-Black Mountain volcanism within the Great Basin. Second, additional age dating of Black Mountain volcanic rocks is needed to adequately define the duration of Black Mountain volcanism. And third, regional patterns of post-Black Mountain volcanism (post-Thirsty Canyon tuff) within the Great Basin need to be determined with respect to age and tectonic setting of the respective volcanic rocks.

#### REFERENCES CITED

- Armstrong, R. L., Dick, Henry, and Vitaliano, C. J., 1972, K-Ar dates and strontium isotope ratios of some Cenozoic volcanic rocks from west-central Nevada: *Isochron/West*, no. 3, p. 23-28.
- Barker, D. S., 1977, Northern Trans-Pecos magmatic province: Introduction and comparison with the Kenya Rift: *Geological Society of America*, v. 88, no. 10, p. 1428-1436.
- Byers, F. M., Jr., Carr, W. J., Orkild, P. P., Quinlivan, W. D., and Sargent, K. A., 1976, Volcanic suites and related cauldrons of the Timber Mountain-Oasis Valley caldera complex, southern Nevada: *U.S. Geological Survey Professional Paper 919*, 70 p.
- Christiansen, R. L., Lipman, P. W., Carr, W. J., Byers, F. M., Jr., Orkild, P. P., and Sargent, K. A., 1977, Timber Mountain-Oasis Valley caldera complex of southern Nevada: *Geological Society of America Bulletin*, v. 88, no. 7, p. 943-959.
- Christiansen, R. L., and Noble, D. C., 1965, Black Mountain volcanism in southern Nevada [abs.]: *Geological Society of America Special Paper 82*, p. 246.
- \_\_\_\_\_, 1968, Geologic map of the Trail Ridge Quadrangle, Nye County, Nevada: *U.S. Geological Survey Geologic Quadrangle Map GQ-774*.
- Ekren, E. B., 1968, Geologic setting of Nevada Test Site and Nellis Air Force Range, in E. C. Eckel, ed., *Nevada Test Site: Geological Society of America Memoir 110*, p. 11-19.
- Ekren, E. B., Anderson, R. E., Rogers, C. L., and Noble, D. C., 1971, *Geology of northern Nellis Air Force Base Bombing and Gunnery Range, Nye County, Nevada: U.S. Geological Professional Paper 651*, 91 p.
- Kistler, R. W., 1968, Potassium-argon ages of volcanic rocks in Nye and Esmeralda Counties, Nevada, in E. C. Eckel, ed., *Nevada Test Site: Geological Society of America Memoir 110*, p. 251-261.
- Kolstad, C. D., and McGetchin, T. R., 1978, Thermal evolution models for the Valles Caldera with reference to a Hot-Dry-Rock Geothermal Experiment: *Journal of Volcanic and Geothermal Research*, v. 3, p. 197-218.
- Lachenbruch, A. H., Sass, J. H., Munroe, R. J., and Moses, T. H., Jr., 1976, Geothermal setting and simple heat conduction models for the Long Valley caldera: *Journal of Geophysical Research*, v. 81, no. 5, p. 769-784.
- Macdonald, Ray, and Bailey, D. K., 1973, The chemistry of the peralkaline oversaturated obsidians: *U.S. Geological Survey Professional Paper 440-N-1*, p. N1-N37.
- Macdonald, Ray, 1974, Nomenclature and petrochemistry of the peralkaline oversaturated extrusive rocks: *Bulletin of Volcanologie*, v. 38, no. 3, p. 498-516.
- Noble, D. C., 1965, Gold Flat Member of the Thirsty Canyon Tuff--a pantellerite ash-flow sheet in southern Nevada: *U.S. Geological Survey Professional Paper 525-B*, p. B85-B90.
- \_\_\_\_\_, 1968a, Kane Springs Wash volcanic center, Lincoln County, Nevada, in E. C. Eckel, ed., *Nevada Test Site: Geological Society of America Memoir 110*, p. 109-116.
- \_\_\_\_\_, 1968b, Systematic variation of major elements in comendite and pantellerite glasses: *Earth and Planetary Science Letters*, v. 4, p. 167-172.
- \_\_\_\_\_, 1970, Loss of sodium from crystallized comendite welded tuffs of the Miocene Grouse Canyon Member of the Belted Range Tuff, Nevada: *Geological Society of America Bulletin*, v. 81, p. 2677-2687.

- Noble, D. C., Anderson, R. E., Ekren, E. B., and O'Connor, J. T., 1964, Thirsty Canyon Tuff of Nye and Esmeralda Counties, Nevada: U.S. Geological Survey Professional Paper 475-D, p. D24-D27.
- Noble, D. C., Bath, G. D., Christiansen, R. L., and Orkild, P. P., 1968, Zonal relations and paleomagnetism of the Spearhead and Rocket Wash Members of the Thirsty Canyon Tuff, southern Nevada: U.S. Geological Survey Professional Paper 600-C, p. C61-C63.
- Noble, D. C., Sargent, K. A., Mehnert, H. H., Ekren, E. B., and Byers, F. M., Jr., 1968, Silent Canyon volcanic center, Nye County, Nevada: Geological Society of America Memoir 110, p. 65-75.
- Noble, D. C., and Christiansen, R. L., 1968, Geologic map of the southwest quarter of the Black Mountain quadrangle, Nye County, Nevada: U.S. Geological Survey Miscellaneous Geologic Investigations Map I-562.
- Noble, D. C., and Christiansen, R. L., 1974, Black Mountain volcanic center: Nevada Bureau of Mines and Geology Special Report 19, p. 27-34.
- Noble, D. C., and Parker, R. L., 1974, Peralkaline silicic volcanic rocks of the western United States: Bulletin of Volcanologie, v. 38, no. 3, p. 803-827.
- Orkild, P. P., Byers, F. M., Jr., Hoover, D. L., and Sargent, K. A., 1968, Subsurface geology of Silent Canyon caldera, Nevada Test Site, Nevada: Geological Society of America Memoir 110, p. 77-86.
- Orkild, P. P., Sargent, K. A., and Snyder, R. P., 1969, Geologic map of Pahute Mesa, Nevada Test Site, Nye County, Nevada: U.S. Geological Survey Miscellaneous Geologic Investigations Map I-567.
- Orkild, P. P., and Jenkins, E. C., 1970, Report of exploration progress, Pahute Mesa: U.S. Geological Survey Report USGS-474-70, 83 p.
- Poole, F. G., Carr, W. J., and Elston, D. P., 1965, Salyer and Wahmonie Formations of southeastern Nye County, Nevada, in G. V. Cohee and W. S. West, Changes in stratigraphic nomenclature by the U.S. Geological Survey 1964: U.S. Geological Survey Bulletin 1224-A, p. A36-A44.
- Quinlivan, W. D., and Byers, F. M., Jr., 1977, Chemical data and variation diagrams of igneous rocks from the Timber Mountain-Oasis Valley caldera complex, southern Nevada: U.S. Geological Survey Open-file Report 77-724, 9 p.
- Sargent, K. A., Noble, D. C., and Ekren, E. B., 1965, Belted Range Tuff of Nye and Lincoln Counties, Nevada, in G. V. Cohee and W. S. West, Changes in stratigraphic nomenclature by the U.S. Geological Survey 1964: U.S. Geological Bulletin 1224-A, p. A32-A36.
- Sargent, K. A., and Orkild, P. P., 1973, Geologic map of the Wheelbarrow Peak-Rainier Mesa area, Nye County, Nevada: U.S. Geological Survey Miscellaneous Geologic Investigations Map I-754.
- Stewart, J. H., and Carlson, J. E., 1976, Cenozoic rocks of Nevada: Nevada Bureau of Mines and Geology Map 52.